First-principles thermodynamics of transition metals: W, NiAl, and PdTi

Graeme J. Ackland, Xiangyang Huang, and Karin M. Rabe
Department of Physics and Astronomy, Rutgers University, Piscataway, New Jersey 08854-8019, USA
(Received 24 July 2003; published 24 December 2003)

We apply the pseudopotential density-functional-perturbation theory approach along with the quasiharmonic approximation to calculate the thermal expansion of tungsten and two important metallic alloys NiAl and PdTi. We derive the theory for anisotropic crystal structures and test the approximation that the anisotropic effects of thermal expansion are equivalent to negative pressure—this simplifies the calculation enormously for complex structures. Throughout, we find excellent agreement with experimental results.

DOI: 10.1103/PhysRevB.68.214104 PACS number(s): 64.70.Kb, 65.40.−b, 71.15.Nc

I. INTRODUCTION

First-principles calculations have established an excellent record for describing the ground state properties of materials at zero temperature over almost 20 years. More recently, the full description of the electronic structure allows for accurate calculation of phonon frequencies[1] and the thermodynamic properties derivable from them.[2] These methods have been applied to insulating systems and elemental metals. In this paper, we extend the methodology to investigate transition metals and compounds that have a low symmetry or phonon anomalies. Previous authors have looked at elemental metals Al, Li, Na,[3] Ag,[4] Cu,[5] and W (Ref. 6) and found that the quasiharmonic approximation holds most of the way to melting. The quasi-harmonic approximation has also been applied on investigation of the temperature-induced phase transition in tin.[7] Recently, first-principles methods have been used to study anisotropic thermal expansion in silicates.[8] We extend this work to alloys, which introduces some different features. As our prototype materials, we study W, NiAl, and PdTi, which have many similarities but each of which has aspects of peculiar interest.

NiAl is a high melting point alloy, which finds applications in aerospace and turbine blade design. Its electronic structure is characterized by Kohn anomalies in the phonon spectrum,[9] arising from a Fermi-surface nesting effect. A huge amount of work has been done on the system using empirical potentials,[10–14] which cannot describe the Kohn anomaly, and it is interesting to examine whether this neglect has serious structural consequences. Crystallographically, NiAl has the cubic $B2$ (CsCl) crystal structure which is stable at all temperatures. This high symmetry simplifies the electronic structure calculation enormously.

PdTi provides a sharp contrast to NiAl. It is a high-temperature shape memory alloy, isostructural with NiAl at high temperatures in the $B2$ phase, but undergoing a martensitic phase transition to the tetragonal $B19$ phase at 810 K and predicted to undergo a further transition to the monoclinic $B19'$ at very low temperatures.[15] The dynamically stabilized high-temperature phase and low-symmetry low-temperature phase each provides a challenging test for theoretical prediction.

Tungsten is another high melting point transition metal. In addition to studying its own thermal expansion, we use this to investigate the effects of anisotropic strain on the phonon contribution to the free energy. This enables us to make a simple test of some approximations required in the calculation of PdTi.

The difference between the materials being studied is highlighted by the phonon spectra for the $B2$ phase: NiAl and PdTi both adopt the $B2$ structure at high temperature while tungsten is a refractory metal and has a bcc structure at all temperatures. The bcc structure can be regarded as a special case of $B2$ where both atoms are the same. NiAl has phonon anomalies due to Fermi-surface nesting, while $B2$ structure PdTi is dynamically stabilized: it has negative frequency phonons (i.e., mechanically unstable) at low temperatures. Such a situation leads to temperature-dependent modes, which cannot be treated within the quasiharmonic approximation and would need to be dealt with separately either in real[16] or reciprocal[17] space.

The quasiharmonic approximation[18] to the free energy assumes that all phonons can be treated as simple-harmonic oscillators with a frequency dependent on the volume of the material. The static lattice energy ($T=0$) is evaluated at a range of volumes, and for each of these the phonon-dispersion relation is calculated. The quasiharmonic contribution to the free energy at finite temperature is then evaluated from Bose-Einstein statistics of the phonons at a given volume. From this the pressure can be evaluated for all conditions of T and V, giving an equation of state. Alternately in the zero-pressure case, the relationship between T and V (i.e., the thermal expansion) can be determined. Since larger volumes typically lead to lower phonon frequencies, the entropy is typically lowered by expansion. Thus larger volume (entropy) is favored at higher temperatures, and thermal expansion occurs.

There are, of course, other contributions to thermal expansion in ordered alloys (antisite defect creation, vacancy creation, coupling of phonons to lattice parameters, and anharmonic effects due to finite atomic displacements) and it is interesting to test that how much of the observed expansion can be attributed to quasiharmonic effects.

II. THEORY

Phonon dispersions can be evaluated using density-functional-perturbation theory (DFPT) (Ref. 19) and finite displacement methods.[20] Here we use the former. Previous work on isotropic equations of state for cubic materials cov-

 ©2003 The American Physical Society

ers much of the theory, here we investigate the practical requirements for lower-symmetry materials, in particular what approximations can be make to made calculations tractable.

Virtually all implementations of density-functional theory based *ab initio* codes take as input the unit-cell vectors $\mathbf{a},\mathbf{b}$ and $\mathbf{c}$ and atomic positions. We define a matrix B comprised of the three unit-cell vectors:

$$B=(\mathbf{a},\mathbf{b},\mathbf{c}).$$

The volume of the unit cell is

$$V=|B|=(\mathbf{a}\times\mathbf{b})\cdot\mathbf{c}.$$

For a cubic material, the quasiharmonic approximation uses the phonon frequencies calculated at different volume to obtain the free energy as a function of two variables,

$$F(V,T)=E(V)-k_BT\ln Z(V,T), \tag{1}$$

where $E(V)$ is the cold curve energy at the volume V (i.e., the energy of a system with the atoms placed on their lattice sites), k_B is Boltzmann's constant, and Z is the vibrational partition function. We assume that for all temperatures of interest the contribution of electronic excitations is negligible—generally true for equation of states,[21] but not for transport properties such as heat conduction.

From $F(V,T)$ one can obtain the equation of state of the single phase of the system:

$$P=-\left(\frac{\delta F}{\delta V}\right)_T \tag{2}$$

and the volume thermal expansion

$$\alpha_V=\frac{1}{V}\left(\frac{\delta V}{\delta T}\right)_P. \tag{3}$$

These can be evaluated for a given structure regardless of whether an alternate phase of lower Gibbs free energy exists.

For noncubic materials, the free energy is a function of all independent cell parameters, and the linear thermal expansion is a tensor quantity. Calculating the free energy across such a multidimensional space is impractical, so we examine a further approximation, that the effect of increasing temperature is equivalent to a negative pressure.[22] At each pressure value, the internal coordinates must be rerelaxed to their equilibrium position within the unit cell, since the phonon spectrum is only well defined by an expansion about such an equilibrium.

Thus, we proceed as follows:

(1) Evaluate the equilibrium structure at $P=0$, by minimizing $U(\mathbf{a},\mathbf{b},\mathbf{c},\{u_i\})\equiv U_0$ where u_i are the internal atomic coordinates.

(2) Evaluate the force constants and hence the phonon-dispersion relation for the relaxed structure, and the partition function $Z(V,T)$ for these oscillators. $V=|B|=(\mathbf{a}\times\mathbf{b})\cdot\mathbf{c}$.

(3) Evaluate Helmholtz free energy at a range of temperatures $F(V,T)=U_0-k_BT\ln Z(V,T)$.

(4) Evaluate the equilibrium structure at P, $T=0$ by minimizing enthalpy $U(\mathbf{a},\mathbf{b},\mathbf{c},\{u_i\})+PV\equiv H_0(V)$, where u_i are the internal atomic coordinates.

(5) Evaluate the phonon-dispersion relation for this relaxed structure, and the partition function $Z(V,T)$ for these oscillators.

(6) Evaluate Helmholtz free energy at fixed V for a range of temperatures $F(V,T)=U(\mathbf{a},\mathbf{b},\mathbf{c},\{u_i\})-k_BT\ln Z(V,T)$.

(7) Repeat steps 4, 5, and 6 for a range of positive and negative pressures.

Once a coarse grid of V points is generated (for thermal expansion, as few as three different pressures suffices), a finer grid can be generated without further expensive *ab initio* calculation by interpolating force constants.[21] A dense grid of T points can easily be generated at a given V. From $F(V,T)$ it is straightforward to transform to $G(P,T)=F(V,T)-V(\delta F/\delta V)_T$.

In terms of speed and accuracy there is little to choose between DFPT or finite displacements: the former involves calculation of second derivatives and the latter requires large supercells. We note that for finite displacements, once the eigenvectors are calculated at $P=0$, a single calculation of restoring forces with all atoms displaced suffices at other volumes.[2]

The allowed occupation states of each phonon mode of frequency ω are $\epsilon_n(\omega)=(n+1/2)\hbar\omega$, where n is the number of *phonons* populating that mode. The canonical partition function is therefore

$$\xi(\omega)\equiv\sum_{n=0}^{\infty}e^{-\beta\epsilon_n(\omega)}=\frac{1}{2\sinh(\hbar\omega/2k_BT)}. \tag{4}$$

The total partition function is then

$$Z=\Pi_\omega\xi(\omega). \tag{5}$$

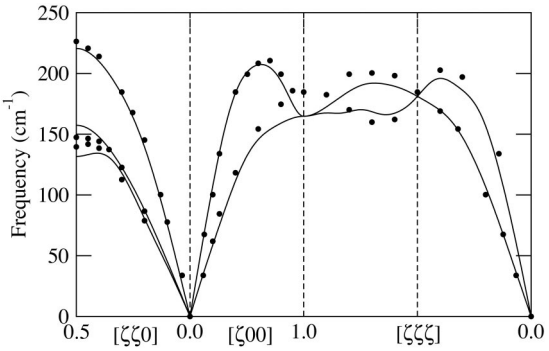

FIG. 1. Phonon spectra calculated for bcc W at $a_0=2.905$ Å, using the PWSCF and PHONON code (Ref. 26) with DFPT (Ref. 27) and a norm conserving pseudopotential. The electronic wave functions were represented in a plane-wave basis set with a kinetic energy cutoff of 32 Ry. The BZ integrations were carried out by the Hermite-Gaussian smearing technique (Ref. 28) using a $16\times16\times16$ k-point mesh. Phonon calculations are exact on meshes which are commensurate with the q-point mesh: a $8\times8\times8$ mesh for tungsten. Other phonons come from dynamical matrices calculated using force constants determined by Fourier transform of original data (Ref. 27).

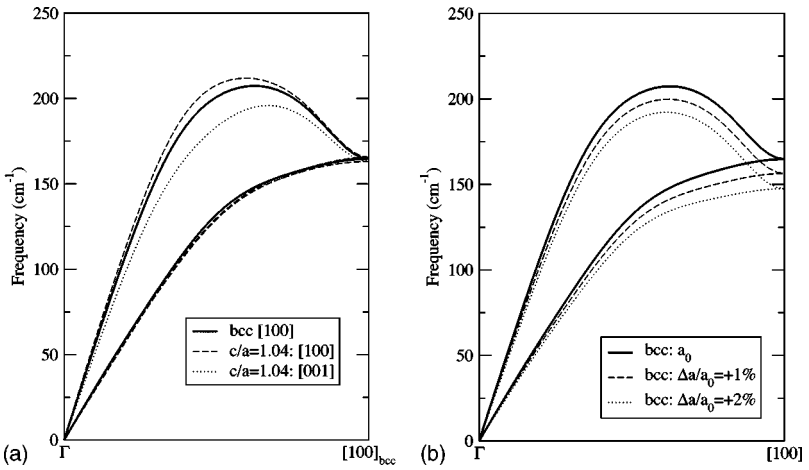

FIG. 2. [001] and [100] branches of the tungsten dispersion relation for (a) volume-conserving strains of 4% on (001) (b) bulk strains of 1% and 2%. The key observation is that for volume-conserving shear some frequencies increase while others decrease, meanwhile for volume expansion all frequencies decrease. Thus in the former case some compensation occurs to keep the phonon free-energy constant, while in the latter case all modes contribute to increase free energy. Calculation details are as for Fig. 1.

For calculating thermal expansion under constant (zero) pressure boundary condition, the essential quantity is the free energy. The mean vibrational free energy

$$-k_B T \ln Z(V,T) = -k_B T \int_0^\infty g(\omega,V) \ln[\xi(\omega,T)] d\omega, \quad (6)$$

introducing the phonon density of states $g(\omega,V)$ to make the dependence of density of states on volume explicit.

Phonon frequencies are evaluated at a dense set of q points in the first Brillouin zone (BZ) using the force constant matrix obtained by fourier transform of the ''exact'' DFPT frequencies. The density of phonon states is calculated by integration using the tetrahedron method.[23] This provides $Z(V,T)$ required in step (2) above.

The structure obtained at a particular temperature and pressure can be found by minimizing the Gibbs free energy with respect to the lattice vectors and internal coordinates of the atoms, ensuring that the solution is a minimum in the combined space of B_{ij} and u_k.[24]

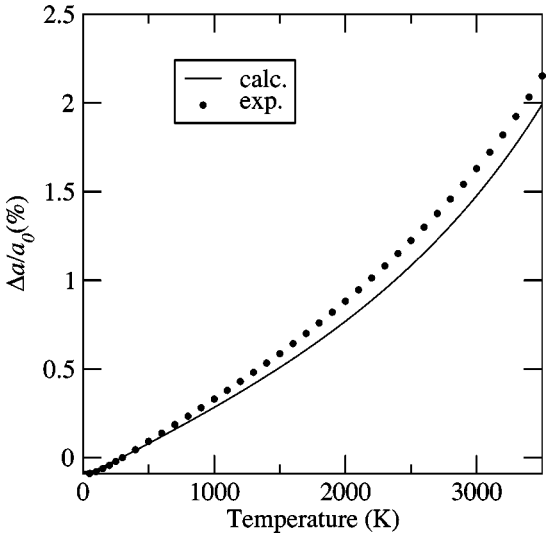

FIG. 3. Calculated linear thermal expansion for tungsten, compared with experimental data from Ref. 29. a_0 represents the room-temperature volume.

$$\frac{dG}{dB_{ij}} = 0, \quad \frac{dG}{d\mathbf{u_k}} = 0. \quad (7)$$

These derivatives can be split into cold curve $[H(B,\mathbf{u_k})]$ and phonon (G_{phon}) contributions.

To make calculations for complex structures tractable, we make the assumption that the phonon part of the free energy is a function of volume *only*, and is independent of $\mathbf{u_k}$. We examine this approximation in the case of anisotropic deformation of tungsten and find it to be good. Intuitively, this can be understood if the force constants vary linearly with separation: we might expect that volume-conserving shears and changes in $\mathbf{u_k}$ will stiffen some force constants and weaken others, raising some frequencies and lowering others to give an overall cancellation in the small strain limit. By contrast, volume increases weaken all force constants and give a systematic decrease in mean frequency. Hence the conditions above become

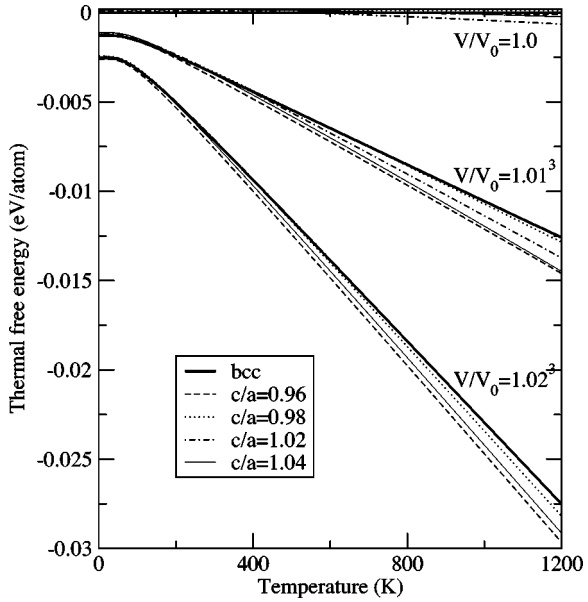

FIG. 4. Graphs of tungsten phonon free energy against temperature for 15 different strain conditions, plotted relative to $G(V,T=0)$ for V at the cold-curve minimum. The effect of volume strain can be seen to be about ten times greater than that of shear strain.

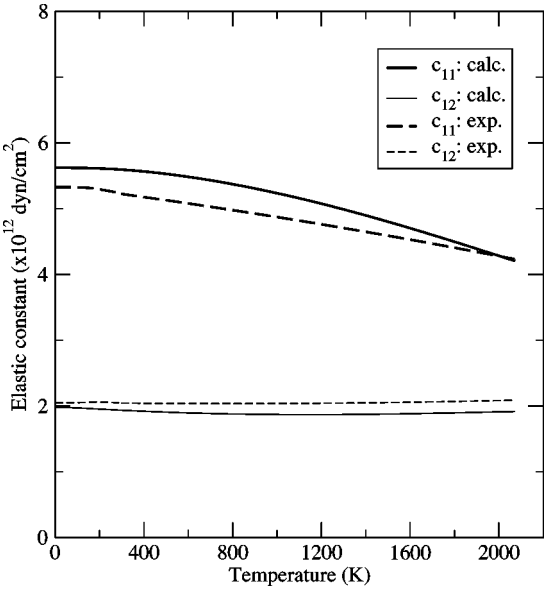

FIG. 5. Calculated elastic constants c_{11} and c_{12} for tungsten, compared with experimental data from Ref. 30. The constant value of c_{12} is well reproduced: it arises from cancellation of a number of terms, and is not generally observed in transition metals.

$$\left.\frac{\partial H}{\partial B_{ij}}\right|_{\mathbf{u_k}} = 0, \tag{8}$$

$$\left.\frac{\partial G_{phon}}{\partial V}\right|_{\mathbf{u_k}} = 0, \tag{9}$$

$$\left.\frac{\partial H}{\partial \mathbf{u_k}}\right|_{V} = 0. \tag{10}$$

III. RESULTS

1. Anisotropic strain—Tungsten

We use tungsten as a benchmark to investigate the effects of anisotropic strain on the phonon contribution to the free energy. Tungsten has a bcc crystal structure. The calculations were done with the generalized gradient approximation (GGA) and the equilibrium lattice parameter was computed to be 2.905 Å, comparable to the experimental result of 2.887 Å. Phonon calculations were done at three different volumes: V_0, 1.01^3V_0, and 1.02^3V_0. At each volume, phonon dispersion was done with the bcc structure and tetragonal strained structures with four different c/a ratios, i.e. 0.96, 0.98, 1.02, and 1.04.

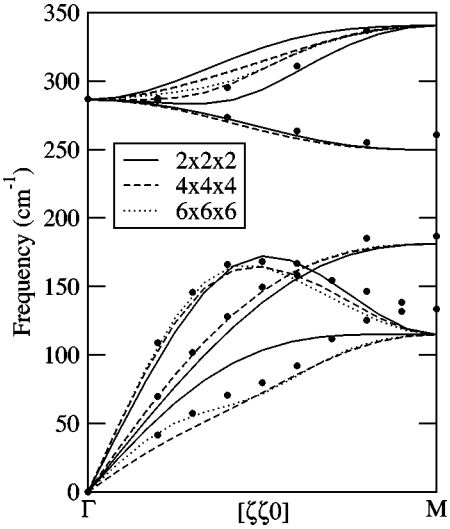

FIG. 6. Phonon-dispersion relations along the acoustic (110) branches in NiAl, calculated with increasing q-point density. Lines are calculated data, taken from force constants deduced from Fourier transforming the $\omega(q)$ data. Labels indicate the number of q points used in the DFPT calculation. Symbols indicate experimental data taken from Ref. 31 for a composition of $Ni_{50}Al_{50}$. Calculations use the PWSCF and PHONON (Ref. 26) code and DFPT (Ref. 27) using an ultrasoft pseudopotentials for Ni (Ref. 32), and a norm conserving pseudopotential for Al. The electronic wave functions were represented in a plane-wave basis set with a kinetic energy cutoff of 30 Ry. The BZ integrations[28] used $12\times12\times12$ mesh for NiAl, giving exact phonon on a $6\times6\times6$ mesh.

We calculated phonon density of states at 15 different structures corresponding to tetragonal strains (e_{xx}; $e_{yy}=e_{zz}$; $e_{xy}=e_{yz}=e_{zx}=0$). The phonon dispersion of bcc tungsten at equilibrium lattice parameter along with experimental results is shown in Fig. 1, while the phonon dispersions under tetragonal strains and a larger volume are shown in Figs. 2(a) and 2(b), respectively. The calculated phonon frequencies are in good agreement with experiment (Fig. 1) and with a recent calculation.[6] Figures 2(a) and 2(b) show that compared to volumetric strain, volume-conserving shear strains have negligible contribution to phonon free energy.

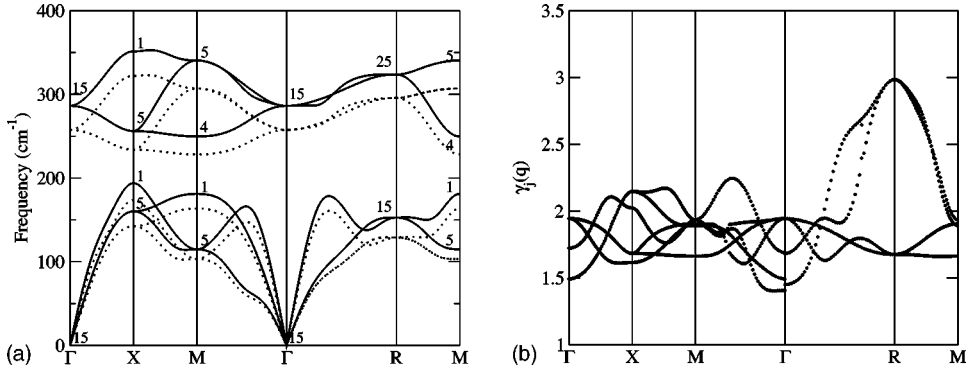

FIG. 7. (a) Phonon spectra calculated for $B2$ NiAl, solid lines are at a lattice parameter of $a_0 = 2.906$ Å (GGA theoretical lattice constant) the dotted lines at a lattice of $1.02a_0$. All phonons have higher frequencies under compression. (b) Calculated mode Grüneisen parameters of NiAl along symmetry lines of simple cubic BZ at equilibrium volume.

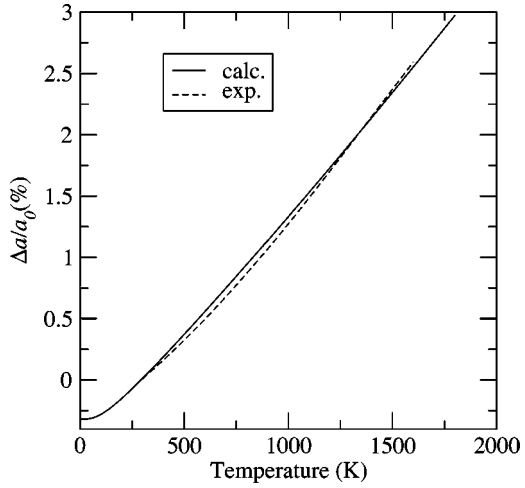

FIG. 8. Calculated thermal expansion for NiAl, compared with experimental data from Ref. 33. The zero of lattice parameter a_0 is chosen to be 2.905 Å in the theory and 2.886 Å in the experimental case, which correspond to 273 K.

The free energy was evaluated at each strain state. In Fig. 3 we show the thermal expansion calculated using the three isotropic strains. The linear thermal expansion adopts the form from Ref. 25. The agreement between theoretical and experimental results is very good.

Figure 4 shows the phonon free energy with different strain. As expected, the phonon contribution to the free energy is only weakly affected by volume-conserving anisotropic strain. Thus it is a good approximation to neglect this term: a given volume-conserving strain contributes about 5% as much as equivalent volume strain.

Using the information from Figs. 3 and 4, we are able to calculate bulk modulus and shear modulus c' as a function of temperature. The elastic constants c_{11} and c_{12} can therefore be obtained. The calculated results along with experimental data are shown in Fig. 5. The experiment shows that c_{11} softens by about 20% when the temperature increases from 0 K to 2073 K while c_{12} remains nearly the same. The excellent agreement between theory and experiment suggests that the quasiharmonic approximation works well in this regime.

2. Anomalous phonons—NiAl

The phonon spectrum of $B2$ NiAl is characterized by Kohn anomalies; as a consequence, to describe the phonon dispersion properly requires a thorough DFPT q-point sampling or (equivalently) large supercells in direct space methods. In Fig. 6, we show the convergence of the result to experimental observation with q-point sampling density.

Despite the anomalies, we find that the thermodynamic properties are almost independent of q-point sampling aside from a rigid shift of the free energy. This does not affect the thermal expansion, but stabilizes the structure slightly against alternate structures because of the increased entropy of the low-frequency phonons.

The entire calculated phonon-dispersion relations at two different volumes are shown in Fig. 7(a). All phonon frequencies increase under compression. Hence the mode Grüneisen parameters $\gamma_j(\mathbf{q})$ shown in Fig. 7(b), and defined as

$$\gamma_j(\mathbf{q}) = -\frac{\partial \omega_j(\mathbf{q})}{\partial V}\frac{V}{\omega_j(\mathbf{q})},$$

are positive throughout the whole BZ. There is no anomalous thermal expansion. Integration of free energies derived from phonon spectra gives the thermal expansion shown in Fig. 8. The excellent agreement with experimental data suggests that both DFPT phonons and the quasiharmonic approximation are valid in this case.

3. Complex structure—PdTi

For PdTi we calculate phonon spectra for two phases, the low temperature $B19'$ and the ambient temperature $B19$ phase. In both cases, the equilibrium cold-curve structure is determined for a particular pressure by relaxing internal parameters and lattice constants simultaneously.[15] It is then assumed that the effect of thermal expansion on lattice-parameter ratios and internal parameters is equivalent to that of (negative) pressure, such that the phonon spectrum need only be evaluated once at each volume, and the free energy can be interpolated as a function of volume only, with the free-parameter relaxation done on the cold-curve structure. The results for anisotropic deformation in tungsten (Fig. 4) suggest that even if the effects of pressure and thermal expansion on free parameters are not equivalent, the consequent change in thermal free energy due to nonvolumetric strains will be small.

The $B19'$ phase has stable phonons throughout the entire BZ [Fig. 9(a)] but the $B19$ phase [Fig. 9(b)] has some imaginary frequency modes: we assume that these contribute to the free-energy-like free particles.[21] Assuming the phonons in the $B19'$ phase to remain harmonic up to and above the

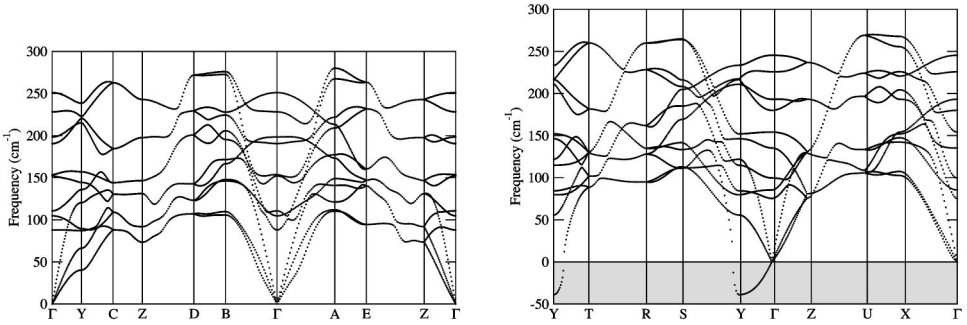

FIG. 9. Phonon spectra calculated for (a) $B19'$ PdTi (b) $B19$ PdTi. $B19$ has many soft phonon modes which characterize the dynamical instability (gray region, these frequencies are actually imaginary). Calculations ultrasoft pseudopotentials (Ref. 32) $12\times8\times8$ mesh and 30-Ry cutoff.

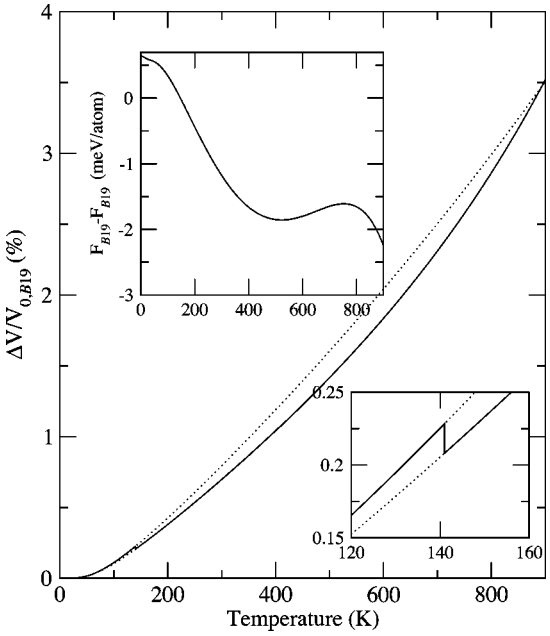

FIG. 10. Calculated percentage thermal expansion for PdTi, including the $B19$-$B19'$ phase transition (expanded scale in lower insert). The dotted lines show the calculated thermal expansion for the thermodynamically unstable phase (B19 at low T, $B19'$ at high T), assuming that all modes remain harmonic. The reference volume is the $T=0$ volume for $B19'$:30.64 Å^3 which is indistinguishable from the equilibrium for B19: 30.64 Å^3 and about 0.34% larger than the cold curve minimum[15] which excludes zero-point vibrations. The upper insert shows the free-energy difference between the two phases as a function of temperature, with the phase transition at 140 K. This is very much larger than the estimate taken from the Landau barrier height (Ref. 15).

phase transition, this enables us to calculate the relative free energies of the two phases, and determine for each temperature not only the lattice parameters but also which is the stable phase. This gives rise to the thermal expansion shown in Fig. 10 with a discontinuity marking the phase transition.

The calculated phase-transition temperature for the $B19$-$B19'$ phase, on the basis of equal quasiharmonic free energies, is 140 K. This can be compared with another estimate based on treating the $B19$ phase as a barrier between equivalent $B19'$ variants, which barrier (about 0.0007 eV/atom) can continually be crossed when the temperature reaches $\Delta E/k_B=9$ K in the higher-temperature phase. The discrepancy between these arises because one concentrates on dynamics of a particular soft mode, while the other considers the static average over all modes: experimentally, the lower of the two is expected.

IV. DISCUSSION

We have calculated the thermal-expansion properties of W, NiAl, and PdTi using the quasiharmonic approximation and DFPT finding that agreement with the experiment is excellent. This shows that the harmonic phonon free energy is by far the dominant effect in thermal expansion, and that other effects such as thermal defects, electron free energy, coupling of phonons to lattice parameters, and anharmonic effects due to finite atomic displacements can safely be neglected.

These three materials are chosen to represent an increasingly challenging test to this methodology. The accurate thermal expansion in tungsten was expected on the basis of previous work,[3,4] and allowed for the demonstration that anisotropic strain has only a second-order effect on the free energy. Similarly the results on NiAl show that the method can be applied to alloys just as effectively as with elements and showed that the presence of phonon anomalies also has little effect on thermal expansion.

Without these two results, the PdTi calculation would have been intractable, but armed with the knowledge that the anisotropic temperature effect can be treated as a pressure effect on the cold curve, allowing the vibrational partition function to be treated as a function of volume only, calculation and minimizations of the full $G(B_{ij},\mathbf{u_k},T)$ becomes tractable. In addition, implementing the previously described treatment of soft phonons[21,17] allow us to predict the thermal expansion of both $B19'$ and the dynamically stabilized $B19$ PdTi crystal, in addition to estimating the phase-transition temperature for $B19$-$B19'$. To our knowledge, these quantities have yet to be measured experimentally and such measurement will provide a sensitive test to our methods.

In sum, this paper represents a significant theoretical advance in the type of materials whose thermal expansion can be calculated from *ab initio* simulation.

This work was carried out under Grant No. AFOSR/MURI F49620-98-1-0433. The calculations were performed on the SGI Origin 2k/3k at ARL MSRC. G.J.A. would also like to acknowledge the Fulbright Foundation for support.

[1] S. Baroni, S. de Gironcoli, A. Dal Corso, and P. Giannozzi, Rev. Mod. Phys. **73**, 515 (2001).
[2] G.J. Ackland, J. Phys.: Condens. Matter **14**, 2975 (2002).
[3] A.A. Quong and A.Y. Liu, Phys. Rev. B **56**, 7767 (1997).
[4] J. Xie, S. de Gironcoli, S. Baroni, and M. Scheffler, Phys. Rev. B **59**, 965 (1999).
[5] S. Narasimhan and S. de Gironcoli, Phys. Rev. B **65**, 064302 (2002).
[6] A. Debernardi, M. Alouani, and H. Dreyss, Phys. Rev. B **63**, 064305 (2001).
[7] P. Pavone, S. Baroni, and S. de Gironcoli, Phys. Rev. B **57**, 10 421 (1998).
[8] A.I. Lichtenstein, R.O. Jones, S. de Gironcoli, and S. Baroni, Phys. Rev. B **62**, 11 487 (2000).
[9] X. Huang, I.I. Naumov, and K.M. Rabe (unpublished).
[10] G.J. Ackland and V. Vitek, in *High Temperature Ordered Intermetallic Alloys III*, edited by C.I. Liu, A.I. Taub, N.S. Stoloff, and C.C. Koch, Mater. Res. Soc. Symp. Proc. **133** (Materials

Research Society, Pittsburg, 1988), Vol. 105.
[11] F. Gao, D.J. Bacon, and G.J. Ackland, Philos. Mag. A **67**, 275 (1993).
[12] Y. Mishin, M.J. Mehl, and D.A. Papaconstantopoulos, Phys. Rev. B **65**, 224114 (2002).
[13] Y. Mishin and D. Farkas, Philos. Mag. A **75**, 169 (1997).
[14] M. Yan, V. Vitek, and S.P. Chen, Acta Mater. **44**, 4351 (1996).
[15] X. Huang, G.J. Ackland, and K.M. Rabe, Phys. Rev. B **67**, 024101 (2003).
[16] W. Zhong, D. Vanderbilt, and K.M. Rabe, Phys. Rev. B **52**, 6301 (1995).
[17] N.D. Drummond and G.J. Ackland, Phys. Rev. B **65**, 184104 (2002).
[18] *Theory of Lattice Dynamics in the Harmonic Approximation*, edited by A.A. Maradudin, E.W. Montroll, G.H. Weiss, and I.P. Ipatova (Academic Press, New York, 1971).
[19] S. Baroni, P. Giannozzi, and A. Testa, Phys. Rev. Lett. **58**, 1861 (1987).
[20] G.J. Ackland, M.C. Warren, and S.J. Clark, J. Phys.: Condens. Matter **9**, 7861 (1997).
[21] D.C. Swift, G.J. Ackland, A. Hauer, and G.A. Kyrala, Phys. Rev. B **64**, 214107 (2001).
[22] There is an alternate possibility that thermal expansion is equivalent to isotropic rescaling the lattice constants, however in general this leads to unphysical nonzero stresses on the cold curve and was rejected.
[23] G. Lehmann and M. Taut, Phys. Status Solidi B **54**, 469 (1972).
[24] X. Huang, K.M. Rabe, and G.J. Ackland, Nat. Mater. **2**, 307 (2003).
[25] R.K. Kirby, T.A. Hahn, and B.D. Rothrock, in *American Institute of Physics Handbook*, edited by D.E. Gray, 3rd ed. (McGraw-Hill, New York, 1972), pp. 4–131.
[26] See S. Baroni, S. de. Gironcoli, A. Dal Corso, and P. Giannozzi, http://www.sissa.it/cm/PWcodes.
[27] P. Giannozzi, S. de Gironcoli, P. Pavone, and S. Baroni, Phys. Rev. B **43**, 7231 (1991).
[28] M. Methfessel and A.T. Paxton, Phys. Rev. B **40**, 3616 (1989).
[29] P.G. Nash, Ceram. Eng. Sci. Proc. **21**, 627 (2000).
[30] *Single Crystal Elastic Constants and Calculated Aggregate Properties: A HANDBOOK*, 2nd ed., edited by G. Simmons and H. Wang (MIT Press, Cambridge, 1978).
[31] M. Mostoller, R.M. Nicklow, D.M. Zehner, C.S. Lui, J.M. Mundenar, and E.W. Plummer, Phys. Rev. B **40**, 2856 (1989).
[32] A.M. Rappe, K.M. Rabe, E. Kaxiras, and J.D. Joannopoulos, Phys. Rev. B **41**, 1227 (1990).
[33] S.A. Nepijko, M. Klimenkov, H. Kuhlenbeck, D. Zemlyanov, D. Herein, R. Schlogl, and H.J. Freund, Surf. Sci. **412/413**, 192 (1998).